1521-009X/50/8/1119–1125$35.00
DRUG METABOLISM AND DISPOSITION

dx.doi.org/10.1124/dmd.121.000813
Drug Metab Dispos 50:1119–1125, August 2022

Commentary

Examining Physiologically Based Pharmacokinetic Model Assumptions for Cross-Tissue Similarity of Activity per Unit of Enzyme: The Case Example of Uridine 5′-Diphosphate Glucuronosyltransferase

Anika N. Ahmed, Amin Rostami-Hodjegan, Jill Barber, and Zubida M. Al-Majdoub

Centre for Applied Pharmacokinetic Research, School of Health Sciences, University of Manchester, Manchester, UK (A.N.A., A.R.-H., J.B., Z.M.A.-M.) and Certara, Simcyp Division, Sheffield, UK (A.R.-H.)

Received December 12, 2021; accepted May 3, 2022

ABSTRACT

The default assumption during in vitro in vivo extrapolation (IVIVE) to predict metabolic clearance in physiologically based pharmacokinetics (PBPK) is that protein expression and activity have the same relationship in various tissues. This assumption is examined for uridine 5′-diphosphate glucuronosyltransferases (UGTs), a case example where expression and hence metabolic activity are distributed across various tissues. Our literature analysis presents overwhelming evidence of a greater UGT activity per unit of enzyme (higher k_{cat}) in kidney and intestinal tissues relative to liver (greater than 200-fold for UGT2B7). This analysis is based on application of abundance values reported using similar proteomic techniques and within the same laboratory. Our findings call into question the practice of assuming similar k_{cat} during IVIVE estimations as part of PBPK and call for a systematic assessment of the k_{cat} of various enzymes across different organs. The analysis focused on compiling data for probe substrates that were common for two or more of the studied tissues to allow for reliable comparison of cross-tissue enzyme kinetics; this meant that UGT enzymes included in the study were limited to UGT1A1, 1A3, 1A6, 1A9, and 2B7. Significantly, UGT1A9 (n = 24) and the liver (n = 27) were each found to account for around half of the total dataset; these were found to correlate with hepatic UGT1A9 data found in 15 of the studies, highlighting the need for more research into extrahepatic tissues and other UGT isoforms.

SIGNIFICANCE STATEMENT

During physiologically based pharmacokinetic modeling (in vitro in vivo extrapolation) of drug clearance, the default assumption is that the activity per unit of enzyme is the same in all tissues. The analysis provides preliminary evidence that this may not be the case and that renal and intestinal tissues may have almost 250-fold greater uridine 5′-diphosphate glucuronosyltransferase activity per unit of enzyme than liver tissues.

Introduction

Applications of physiologically based pharmacokinetics (PBPK) over the last 20 years have increased exponentially compared with the rest of pharmacokinetics (El-Khateeb et al., 2021). This has been linked to the ability of PBPK models to extrapolate kinetics beyond the average patient by using fundamental aspects of the biology related to the change of the expression in enzymes between healthy individuals and various patient groups (Howard et al., 2018).

The default assumption during the in vitro in vivo extrapolation (IVIVE) steps of metabolic information for drug clearance during PBPK is that expression mirrors activity regardless of the location of the enzyme. In other words, the activity per unit of enzyme (k_{cat}) is considered to be the same in various tissues. We wished to examine this common assumption for the case example of uridine 5′-diphosphate glucuronosyltransferase (UGT) enzymes. These enzymes are involved in phase II biotransformation of many drugs, and they are currently the second most common route for primary drug metabolism, responsible for the metabolic clearance of 10%–30% of all drugs (Stingl et al., 2014). This proportion is set to increase, as pharmaceutical companies are intentionally designing new drug candidates that go through non–cytochrome P450 (CYP450) pathways to reduce the burden of CYP450-related drug-drug interactions (DDIs) (Achour et al., 2014).

Previous research has identified the liver as the epicenter of xenobiotic metabolic processes, containing the most diverse and abundant population of drug-metabolizing enzymes (Achour et al., 2014). However, some may argue that the contributions of other key metabolic tissues

This work received no external funding.
No author has an actual or perceived conflict of interest with the contents of this article.
dx.doi.org/10.1124/dmd.121.000813.

ABBREVIATIONS: AZT, zidovudine; BSA, bovine serum albumin; $CL_{int,u}$, unbound intrinsic clearance; CYP450, cytochrome P450; IVIVE, in vitro in vivo extrapolation; k_{cat}, activity per unit of enzyme; Km, substrate concentration at 1/2 V_{max}; LC-MS, liquid chromatography–mass spectrometry; $MgCl_2$, magnesium chloride; MPA, mycophenolic acid; PBPK, physiologically based pharmacokinetics; UDPGA, UDP-glucuronic acid; UGT, uridine 5′-diphosphate glucuronosyltransferase.

involved in drug disposition have been neglected or underestimated. Studies involving extrahepatic metabolism are very limited compared with hepatic metabolism (Scotcher et al., 2016), and to build a clinically realistic model of the human body, the involvement of enzyme kinetics across extrahepatic tissues must be quantified. This is as true of UGTs as of other enzymes. UGT enzymes quantified in the liver do not have a complete set of corresponding expression values in renal and intestinal tissues (Achour et al., 2014; Couto et al., 2020; Al-Majdoub et al., 2021). This highlights the need to generate a reliable dataset for absolute enzyme abundances across the key metabolic organs as a starting point for quantifying tissue-specific enzyme kinetics.

To begin quantifying UGT enzyme kinetics per unit of enzyme, absolute abundance for individual UGT isoforms must be determined as amount of enzyme per milligram of microsomal protein (Crewe et al., 2011). V_{max}, measurable as amount of isoform-specific probe substrate converted to its metabolite per unit time, must also be determined. The enzyme abundance-activity relationship can then be quantified as k_{cat}, defining the differences in intrinsic activity per unit of UGT. To accurately reflect tissue-specific kinetics, k_{cat} must account for tissue-specific enzyme abundances (Robinson, 2015). The common assumption that k_{cat} is the same across various tissues has not been examined for UGTs, and information on other enzymes is sparse (von Richter et al., 2004; Yang et al., 2004; Galetin and Houston, 2006).

Obviously, the accuracy of clearance predictions will also depend on correct assignment of the extrahepatic metabolism. However, this is not the subject of current exercise. Nonetheless, we make extensive use of the research into the abundance (Achour et al., 2014) and activity of UGT in intestine and kidney even though abundance values are missing for several UGT enzymes (Couto et al., 2020; Al-Majdoub et al., 2021).

Materials and Methods

Collection of Data. Two electronic databases, Web of Science (https://wok.mimas.ac.uk) and PubMed (https://www.ncbi.nlm.nih.gov/pubmed/), were searched for relevant literature from the years 2000 to 2019 using appropriate keywords (UDP-glucuronosyltransferase, UGT activity). Both UGT abundance and activity studies were searched for glucuronidation data; this involved searching for other key terms in place of 'activity' to widen the search scope (glucuronidation, k_{cat}, metabolism, abundance, concentration, content, quantification, measurement, LC-MS, ELISA, Western blotting). Citation lists within the collected studies were also inspected to identify any further relevant literature. Searches were species and tissue-specific for human intestinal and kidney microsomes; keywords included synonyms for these tissues (gut, renal). The search criteria were repeated for human liver microsomes, focusing on literature using the probe substrates identified in renal and intestinal studies, to compile a database of comparable data. All but one publication included data from 'adult' populations; hence only data generated from adult tissue samples were included for analysis.

Calculation of Enzyme Activity. The k_{cat} values for individual UGT isoforms were calculated using eq. 1, where V_{max} represents the maximal metabolic capacity in pmol/min/mg microsomal protein and UGT abundance is tissue-specific for individual isoforms in pmol UGT/mg protein:

$$k_{cat}(\text{pmol/min/pmol UGT}) = V_{max}(\text{pmol/min/mg protein})/\text{UGT abundance (pmol UGT/mg protein)} \quad (1)$$

Where V_{max} was not specified for activity, Km values (substrate concentration at 1/2 V_{max}) were identified for the probe substrates; if the probe concentration (μM) was found to be significantly above the maximum Km value (μM) (i.e., >2-fold), the assumption was made that the reaction was conducted at V_{max} and these data were used to calculate k_{cat}. On the other hand, if the probe concentration (μM) was found to be significantly below the minimum Km value (μM) (i.e., <0.5-fold), the assumption was made that the activity value was within the intrinsic clearance range and the clearance was used as a supplementary measurement of enzyme activity. Here, the literature was examined to identify reported probe Km values, and where this information was not available, reference Km values were found (Seo et al., 2014; Miners et al., 2021). We have to acknowledge that our assumption will result in significant errors in the calculation of these parameters depending on how far the substrate concentrations deviate from those related to initial rate [in which case, UGT intrinisc clearance ($CL_{int,UGT}$) = V_{max}/(Km)] and V_{max}. However, the error introduced by this approach will be less than that associated with the comparison of kinetic data from studies that used vastly different experimental conditions. Where necessary, intrinsic clearance data were corrected for the microsomal fraction of unbound drug to give unbound intrinsic clearance ($CL_{int,u}$) a closer estimate for in vivo clearance (Hallifax and Houston, 2006; Gao et al., 2008). Once the corrected clearance values had been determined, $CL_{int,u}$ (μl/min/mg microsomal protein) values were divided by the abundance (pmol/mg protein) and probe concentrations (μM) to give $CL_{int,u}$ per unit enzyme (μl/min/pmol enzyme).

Results

Filtering Data. A total of 19 studies were used in this analysis; 15 of these were relevant for calculating k_{cat} (Soars et al., 2001, 2003; Miles et al., 2005; Picard et al., 2005; Al-Jahdari et al., 2006; Shimizu et al., 2007; Benoit-Biancamano et al., 2009; Rowland et al., 2008; Komura and Iwaki, 2011; Liang et al., 2011; Walsky et al., 2012; Gill et al., 2013; Knights et al., 2016; Achour et al., 2017, 2018; Chen et al., 2018), whereas the remaining four were used for calculating $CL_{int,u}$ (Cubitt et al., 2009; Gill et al., 2012; Scotcher et al., 2017; Bhatt et al., 2019). Of the total dataset, 29% of the data did not meet the search criteria and were excluded on account of the following: no probe specificity, no availability of abundance data, or not falling into the V_{max} or intrinsic clearance range. The data useful in this analysis are summarized in Table 1. Probes were selected based on availability of data across two or (preferably) all of the studied tissues; because data were very limited, it was necessary to focus on availability rather than specificity of probes. Data were available for UGT1A1, 1A6, 1A9, and 2B7 for k_{cat} calculations. Only UGT1A6, with probe substrate deferiprone, was comparable across all three tissues (Benoit-Biancamano et al., 2009; Knights et al., 2016); UGT1A1 was comparable across the liver

TABLE 1

Summary of the activity data available for analysis (k_{cat} and $CL_{int,u}$ data combined) with a sum total of data for each probe-specific UGT enzyme and a sum total of data for each tissue

Enzyme	Probe	Liver	Intestine	Kidney	n = Total Data for Each Enzyme
UGT1A1	Ezetimibe	2	2	1	5
UGT1A3	Telmisartan	1	1	1	3
UGT1A6	Deferiprone	1	1	2	4
UGT1A9	Propofol	12	0	5	17
UGT1A9	MPA	4	0	3	7
UGT2B7	AZT	3	0	1	4
UGT2B7	Naloxone	4	2	2	8
Total		27	6	15	48

TABLE 2

Mean abundance values from the literature for UGT isoforms across human liver, intestine, and kidney microsomes (pmol/mg protein)

UGT Isoform	1A1[a]	1A3[a]	1A4	1A6[a]	1A9[a]	2B4	2B7[a]	2B10	2B15	2B17	Literature
Liver	41	31.4	55.4	40	32	57	87	20	52	18	(Achour et al., 2014)
Intestine	1.87	1.14	—	0.75	—	—	1.34	—	0.37	—	(Couto et al., 2020)
Kidney	0.14	0.14	0.2	0.25	2.62	—	1.52	—	—	—	(Al-Majdoub et al., 2021)

[a]Useful for calculating k_{cat} and $CL_{int,u}$ based on availability of data on common probes and activity across two or more of the tissues identified in the literature.
—, No data.

and intestine (Komura and Iwaki, 2011); and data for UGT1A9 and 2B7 were comparable across the liver and kidney (Miles et al., 2005; Komura and Iwaki, 2011; Knights et al., 2016). Intrinsic clearance calculations allowed for comparison of UGT1A1 and 1A3 across all three tissues using probe substrates ezetimibe and telmisartan, respectively (Gill et al., 2012); UGT1A9 data were comparable across the liver and kidney (Gill et al., 2012; Scotcher, et al., 2017; Bhatt et al., 2019); and data for UGT2B7 were comparable across the liver and intestine (Gill et al., 2012).

Reference Abundance Values. The collated reference abundance values (Achour et al., 2014; Couto et al., 2020; Al-Majdoub et al., 2021), presented in Table 2, were used to perform k_{cat} and $CL_{int,u}$ calculations, where activity data did not have corresponding abundance values presented in the literature (Soars et al., 2001, 2003; Miles et al., 2005; Picard et al., 2005; Al-Jahdari et al., 2006; Shimizu et al., 2007; Benoit-Biancamano et al., 2009; Rowland et al., 2008; Cubitt et al., 2009; Komura and Iwaki, 2011; Liang et al., 2011; Gill et al., 2012, 2013; Walsky et al., 2012; Scotcher et al., 2017; Chen et al., 2018).

UGT isoforms included in the analysis were based on availability of common probes and activity data (at V_{max}) across two or more of the tissues (UGT1A1, 1A3, 1A6, 1A9, and 2B7); however, a wider range of enzyme expressions are demonstrated in Table 2 to highlight data availability across tissues.

Correlation of UGT Expression and Activity between Different Tissues. The reported activity values for human liver, intestinal, and kidney microsomes used to calculate k_{cat} and $CL_{int,u}$ are demonstrated in Tables 3 and 4, respectively. Some assumptions for V_{max} were made for data used for calculating mean k_{cat} (Table 3), where V_{max} was not specified but probe concentration was found to be more than 2-fold greater than the substrate Km (Knights et al., 2016). Similarly, for $CL_{int,u}$ calculations, where activity data were not specified as V_{max}, it was assumed to be in the intrinsic clearance range if probe concentration was found to be less than 0.5-fold of the substrate concentration (Bhatt et al., 2019). Where activity was assumed to be at V_{max} or intrinsic clearance, probe substrate concentration and Km have also been recorded. Probe concentration was recorded across all $CL_{int,u}$ enzymes to calculate $CL_{int,u}$ per unit enzyme (see *Materials and Methods*). Key experimental differences that may have influenced the activities seen across the studies are recorded in Table 5.

To demonstrate the differences in the mean relative expressions and activities of UGT enzymes across the tissues, scatter graphs were generated with the *y*-axis in logarithmic scale (log_{10}), demonstrating the ratio of fold difference of intestinal and renal abundances and activities relative to the liver (Figs. 1 and 2). Data for enzyme activities were segregated for k_{cat} and $CL_{int,u}$ (Fig. 2, A and B). The reference line for the liver crosses the *y*-axis horizontally at 1; values above or below the line represent greater or fewer enzyme expression, respectively, found in the intestine and kidneys than that found in the liver.

Discussion

This analysis uniquely reviews a comprehensive list of all significant UGT activity studies conducted using comparable probe substrates for

TABLE 3

V_{max} (pmol/min/mg microsomal protein) and calculated k_{cat} (pmol/min/pmol enzyme) data for UGT enzymes using probe substrates across human liver, intestine, and kidney tissues

	Probe		Liver		Intestine		Kidney		
Enzyme/ Identified Probe	*Conc.* (μM)	*Km* (μM)[a]	V_{max}	k_{cat}	V_{max}	k_{cat}	V_{max}	k_{cat}	Study
UGT1A1 *Ezetimibe*	—	—	4400	107	3020	1610	—	—	(Komura and Iwaki, 2011)
UGT1A6 *Deferiprone*	—	—	19,300	483	1250	1670	14,800	59,200	(Benoit-Biancamano et al., 2009)
	20,000	4000[b]	—	—	—	—	21,000	4470	(Knights et al., 2016)
UGT1A9 *Propofol*	—	—	2420	65.3	—	—	—	—	(Achour et al., 2017, 2018)
	—	—	2400	75.0	—	—	7970	3040	(Al-Jahdari et al., 2006)
	—	—	610	19.1	—	—	—	—	(Chen et al., 2018)
	—	—	1390	43.4	—	—	4310	1650	(Gill et al., 2013)
	500	125[b]	—	—	—	—	5660	92.3	(Knights et al., 2016)
	—	—	580	18.1	—	—	—	—	(Liang et al., 2011)
	—	—	1050	32.8	—	—	—	—	(Rowland et al., 2008)
	—	—	1400	43.8	—	—	—	—	(Shimizu et al., 2007)
	—	—	90	2.81	—	—	5800	2210	(Soars et al., 2001)
	—	—	3800	119	—	—	—	—	(Soars et al., 2003)
	—	—	780	24.4	—	—	—	—	(Walsky et al., 2012)
UGT1A9 *MPA*	—	—	14,200	444	—	—	—	—	(Komura and Iwaki, 2011)
	—	—	20,500	641	—	—	—	—	(Miles et al., 2005)
	—	—	5160	161	—	—	12,900	4940	(Picard et al., 2005)
UGT2B7 *AZT*	—	—	1120	14.5	—	—	—	—	(Achour et al., 2017, 2018)
	—	—	90	1.03	—	—	—	—	(Chen et al., 2018)
	5000	1000[b]	—	—	—	—	1230	32.7	(Knights et al., 2016)
	—	—	4700	54.0	—	—	—	—	(Walsky et al., 2012)
UGT2B7 *Naloxone*	—	—	480	5.52	—	—	2000	1320	(Soars et al., 2001)

[a]Where activity is not specified as V_{max} or $CL_{int,u}$, if probe concentration is significantly above the Km value (>2-fold), activity was assumed to be at V_{max}.
[b](Knights et al., 2016).
—, No data.

TABLE 4

$CL_{int,u}$ (μl/min/mg microsomal protein) and calculated $CL_{int,u}$ per unit enzyme (μl/min/pmol enzyme) data for UGT enzymes using probe substrates across human liver, intestine, and kidney tissues

Enzyme/ Identified Probe	Probe		Liver		Intestine		Kidney		Study
	Conc. (μM)[a]	*Km* (μM)[b]	Activity	$CL_{int,u}$	Activity	$CL_{int,u}$	Activity	$CL_{int,u}$	
UGT1A1 *Ezetimibe*	1	—	5180	126	1160	620	495	3540	(Gill et al., 2012)
UGT1A3 *Telmisartan*	1	—	395	12.6	91.4	80.2	34.3	245	(Gill et al., 2012)
UGT1A9 *Propofol*	20	98–127[c]	603[d]	1.67	—	—	—	—	(Bhatt et al., 2019)
	5	—	201	1.26	—	—	1020	78.1	(Gill et al., 2012)
UGT1A9 *MPA*	1	—	233	7.28	—	—	1370	523	(Gill et al., 2012)
	1	—	—	—	—	—	1060	405	(Scotcher et al., 2017)
UGT2B7 *Naloxone*	10	423–870[e]	59.6[d]	0.163	—	—	—	—	(Bhatt et al., 2019)
	1	—	17.4	0.200	21.4	16.0	—	—	(Cubitt et al., 2009)
	1	—	55.6	0.639	14.2	10.6	52.7	34.7	(Gill et al., 2012)

[a]Probe concentration used to calculate $CL_{int,u}$ per unit enzyme (see *Materials and Methods*).
[b]Where activity is not specified as V_{max} or $CL_{int,u}$, if probe concentration was significantly below the Km value (<0.5-fold), activity was assumed to be in the intrinsic clearance range.
[c](Miners et al., 2021).
[d]Activity after correction for fraction drug unbound in the microsomal incubation (fu_{mic})(Hallifax and Houston, 2006; Gao et al., 2008).
[e](Seo et al., 2014).
—, No data.

human liver, intestinal, and kidney microsomal tissues from 2000 to 2019. Nevertheless, it only provides a preliminary database of mean activity values, as k_{cat} and $CL_{int,u}$, for comparable UGT isoforms for the three major metabolic organs since the functional assays were not conducted in the same laboratory nor under exactly similar conditions. We were able to map a ratio of fold difference for the intestine and kidney relative to liver for UGT enzyme abundance but more importantly activity per unit of enzyme. The intestinal and kidney abundance data, which we used for calculating activity per unit of enzyme, were all taken from a single laboratory (University of Manchester; Table 2). A meta-analysis conducted by Achour et al. (2014) presented weighted average abundance values for liver from data published between 1980 and 2014 that were measured using liquid chromatography–mass spectrometry (LC-MS) proteomics and that were used for calculating k_{cat} values in liver. Mean renal and intestinal (from kidney cortex) abundance data were taken from recent studies (Couto et al., 2020; Al-Majdoub et al., 2021), respectively, using the same laboratory environments, LC-MS technology, and consistent assay conditions. Consistency in LC-MS–based quantification across the three studies with abundance reported in the microsomal fraction (pmol/mg microsomal protein) provides a reliable source of reference abundance values. This degree of consistency in abundance values used for the calculation of cross-tissue enzyme kinetics has not been accomplished in any other UGT activity study; it also provides a reference point for cross-tissue UGT enzyme expressions for future research.

Our major objective in this analysis was to explore the assumption of similarity in k_{cat} for UGT enzymes across the liver, intestine, and kidneys, as a case example. Because there is limited research into UGT functional assays involving full kinetics (at different concentrations), we could not calculate k_{cat} in many cases and used $CL_{int,u}$ per unit enzyme instead (measured at low concentrations of the probe). We focused on data for probes that were common for functional assays conducted in at least two of the tissues. Accordingly, the analysis was limited to UGT1A1, 1A3, 1A6, 1A9, and 2B7. Among these, UGT1A9 ($n = 24$) and the liver ($n = 27$) comprised almost half of the data for the analysis (Soars et al., 2001, 2003; Miles et al., 2005; Picard et al., 2005; Al-Jahdari et al., 2006; Shimizu et al., 2007; Rowland et al., 2008; Komura

TABLE 5

Interlaboratory differences between the literatures used for V_{max} and intrinsic clearance data for k_{cat} and $CL_{int,u}$ calculations, including concentrations of UDPGA, alamethicin, $MgCl_2$, and % of BSA

Literature	UDPGA (mM)[a]	Alamethicin[b]	$MgCl_2$ (mM)[b]	BSA (%)[c]	Buffer[d]
(Achour et al., 2018)	5	10μg/ml	5	—	100mM Tris-HCl, pH 7.5
(Al-Jahdari et al., 2006)	3	50μg/ml	8	—	50mM Tris-HCl, pH 7.6
(Benoit-Biancamano et al., 2009)	2	—	10	—	50mM Tris-HCl, pH 7.7
(Bhatt et al., 2019)	2.5	100μg/ml	—	0.01	100mM phosphate, pH 7.4
(Chen et al., 2018)	—	25mg/ml	5	—	50mM Tris-HCl, pH 7.4
(Cubitt et al., 2009)	5	50μg/ml	10	—	100mM phosphate, pH 7.1
(Gill et al., 2012)	5	50μg/mg protein	3.45	1 to 2[e]	100mM phosphate, pH 7.1
(Gill et al., 2013)	5	50μg/ml	3.45	—	100mM phosphate, pH 7.1
(Knights et al., 2016)	5	50μg/mg protein	4	—	100mM phosphate, pH 7.4
(Komura and Iwaki, 2011)	2	50μg/mg protein	10	—	100mM Tris-HCl, pH 7.4
(Liang et al., 2011)	5	25μg/ml	5	—	50mM Tris-HCl, pH 7.4
(Miles et al., 2005)	3	50μg/mg protein	10	—	75mM Tris-HCl, pH 7.45
(Picard et al., 2005)	2	—	10	—	100mM Tris-HCl, pH 7.4
(Rowland et al., 2008)	5	50μg/mg protein	4	—	100mM phosphate, pH 7.4
(Scotcher et al., 2017)	5	50μg/mg protein	3.45	1	100mM phosphate, pH 7.4
(Shimizu et al., 2007)	3	50μg/ml	10	—	50mM Tris-HCl, pH 7.4
(Soars et al., 2001)	5	—	10	—	100mM Tris-maleate, pH 7.4
(Soars et al., 2003)	5	50μg/ml	1	—	100mM phosphate, pH 7.1
(Walsky et al., 2012)	5	10μg/ml	5	—	100mM Tris-HCl, pH 7.5

[a]Minimum 5mM required for reliable glucuronidation activities for k_{cat} and $CL_{int,u}$ calculations (Miners et al., 2021).
[b]Factors influencing measured V_{max} specifically (Miners et al., 2021).
[c]Reduces substrate Km, impacting on measured $CL_{int,u}$ (Miners et al., 2021).
[d]Increases glucuronidation activities, reflected as greater mean $CL_{int,u}$ (Badée et al., 2019).
[e]UGT1A1, 2% BSA; UGT1A3, 1% BSA.
—, No data.

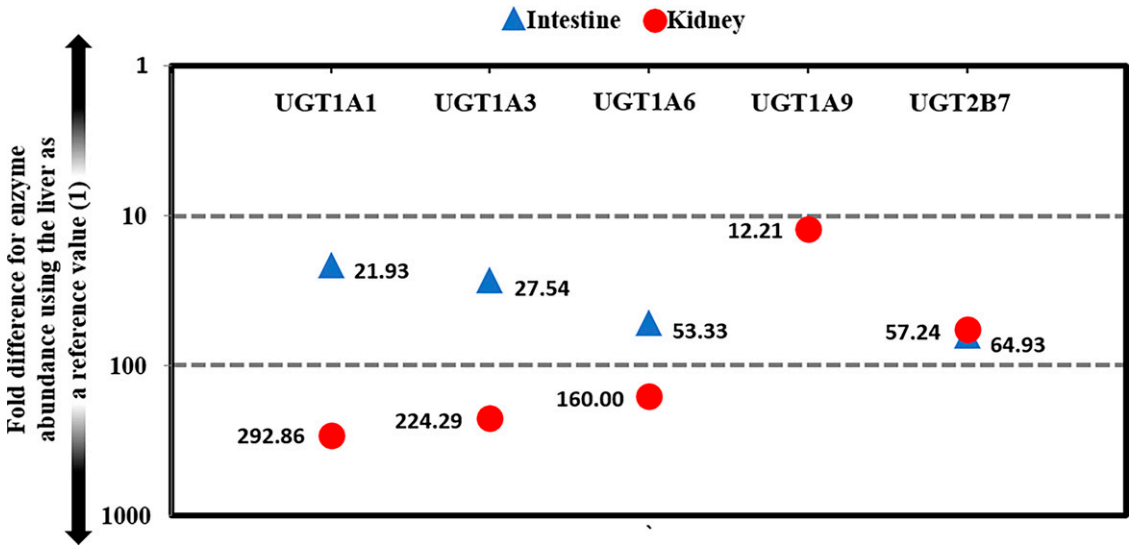

Fig. 1. Comparison of abundance values for UGT enzymes in the gut and kidney as a ratio to the liver. The liver has been used as a reference point, crossing the *y*-axis horizontally at 1. Plotting the *y*-axis in logarithmic scale (log10) demonstrates the fold difference in abundance for intestinal and renal tissues with respect to the liver (specific fold values labeled on the graph).

and Iwaki, 2011; Liang et al., 2011; Gill et al., 2012, 2013; Walsky et al., 2012; Achour et al., 2018; Chen et al., 2018; Bhatt et al., 2019), emphasizing the paucity of functional assays conducted in extrahepatic tissues for majority of UGT isoforms.

Although UGT abundances are unsurprisingly greater within the liver across all measured isoforms (Fig. 1), activity per unit of enzyme appears to be lower in the liver than in the other tissues. There was an overall trend when UGT functional activities were available across all three tissues [UGT1A6 (k_{cat}), 1A1, 1A3, and 2B7 ($CL_{int,u}$)]. These results therefore suggest that the relative contribution of drug metabolism by liver may have been assigned incorrectly for UGT substrates. This is when PBPK models assume the same metabolic clearance by UGT per unit of enzyme in various tissues. A renal k_{cat} of more than 200-fold greater than the liver (e.g., UGT2B7) can compensate greatly for a 300-fold lower abundance relative to liver (e.g., UGT1A1).

Contribution of any enzyme to overall kinetics also depends on other factors such as the blood flow to the organ and the topological arrangements related to the physiology and anatomy (Nishimura et al., 2007; Pang et al., 2019). In addition, enzyme-specific cofactors [e.g., UDP-glucuronic acid (UDPGA) is a glucuronic donor in glucuronidation reactions] are critical. Lack of UDPGA, which needs to be at least 5 mM for optimum glucuronidation activity, and simplification of kinetic analyses leads to loss of activity in all UGT isoforms. Although specific probe substrates have in fact been identified for UGT enzymes (Miners et al., 2021), the analysis in the current study was limited by the lack of enzyme activity data measured using these specific probe substrates—a common research gap for non-CYP450 enzymes (Argikar et al., 2016). Hence, the data in this study were limited by the nonspecificity of some of the probes used for measuring activity (i.e., ezetimibe and naloxone), as data were selected based on availability of comparable probes across the studied tissues. Nevertheless, most of the isoforms could be assessed with confidence using specific probe data: UGT1A3, 1A6, 1A9, and 2B7 using telmisartan, deferiprone, propofol, mycophenolic acid (MPA), and zidovudine (AZT), respectively (Miners et al., 2021). For the remaining UGT enzymes, there is a clear research gap. For instance, although UGT1A9 activity values were available for hepatic, intestinal, and renal tissues as both V_{max} and $CL_{int,u}$, there was a lack of intestinal abundance data and k_{cat} and $CL_{int,u}$ (per unit enzyme) could not be calculated across all organs (Picard et al., 2005; Shimizu et al., 2007; Komura and Iwaki, 2011; Gill et al., 2012, 2013).

Consistency between the protocols measuring the functional activity is another issue that hampers the robust assessment of the k_{cat} across the tissues based on literature data (Table 5). The requirement for a minimum concentration of UDPGA of 5mM (Miners et al., 2021) was met in only half of the studies (Soars et al., 2001, 2003; Rowland et al., 2008; Cubitt et al., 2009; Liang et al., 2011; Gill et al., 2012, 2013; Walsky et al., 2012; Scotcher et al., 2017; Achour et al., 2018). Factors known to affect V_{max} include the concentration of alamethicin in the incubation buffer and the time of preincubation of human tissue microsomes with alamethicin, concentration of magnesium chloride ($MgCl_2$), and choice of organic solvent used for aglycone solubilization in the incubation medium (Miners et al., 2021). Thus, differences in these assay conditions across the studies (Table 5) were expected to have an impact on calculated k_{cat} (Table 3). Bovine serum albumin (BSA) binds free fatty acids that inhibit UGT activity and is therefore frequently included as a component of incubation buffers. Its presence usually results in an increase in measured intrinsic clearance (fraction unbound) for UGT1A9 and UGT2B7 substrates as a result of reduction in the Km (Wu et al., 2013). However, BSA levels were inconsistent across the protocols for assessing functional activity of UGT (Table 5), which may have reduced accuracy in calculated $CL_{int,u}$ (Table 4). Badée et al. (2019) showed that mean $CL_{int,u}$ values are dependent on the nature and concentration of the buffer, with reduced buffer concentration seen to reduce the rate of glucuronidation. Table 5 shows the buffers used in studies cited here. Despite these interlaboratory differences, the trends seen in this analysis are consistent in showing greater glucuronidation activities across the intestinal and kidney tissues than the liver (Fig. 2, A and B).

The abundance measurements suffered much less from these concerns. We were able to use proteomic measurements generated in a single laboratory in this study, so the general lack of interlaboratory consistency in quantifying intestinal and renal UGT enzymes did not apply in the present study (Couto et al., 2020; Al-Majdoub et al., 2021). Moreover, hepatic data taken from the meta-analysis conducted by Achour et al. (2014) uses literature measuring abundance with LC-MS proteomic technology, much like the intestinal and renal studies, maintaining consistency in the standards used for measuring abundance.

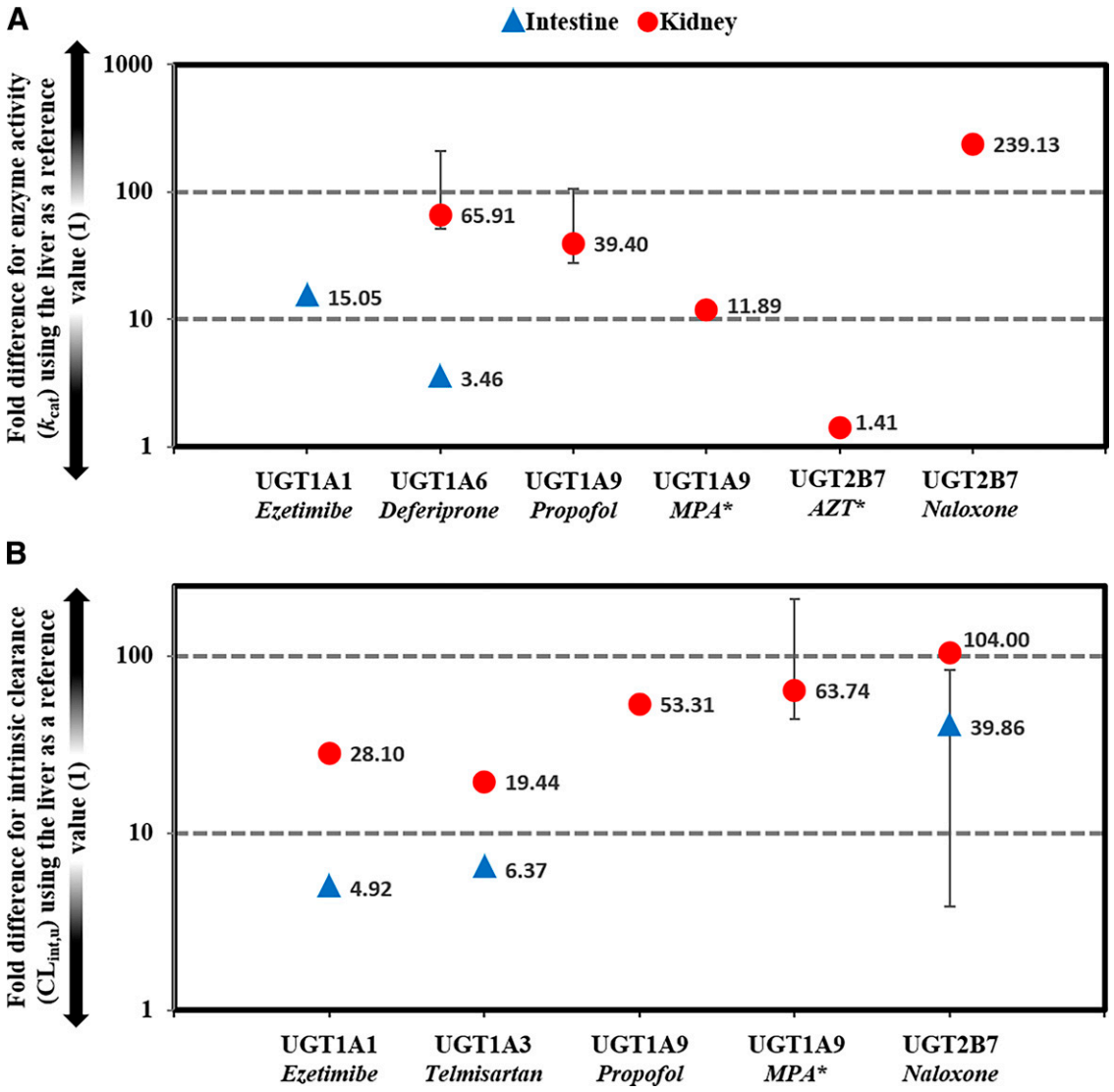

Fig. 2. Comparison of activity values (k_{cat}) (A) and intrinsic clearance ($CL_{int,u}$) (B) for UGT enzymes in the gut and kidney as a ratio to the liver. The liver has been used as a reference point, crossing the *y*-axis horizontally at 1. Plotting the *y*-axis in logarithmic scale (log10) demonstrates the fold difference in abundance for intestinal and renal tissues with respect to the liver (fold values labeled specifically on the graph). Error bars are included where there is sufficient data (i.e., ≥2 data sets).

Going forward, it is imperative to develop and use standardized experimental conditions for future UGT enzyme kinetic research to generate reliable cross-study comparisons.

In conclusion, this preliminary analysis provides a starting point for building tissue-specific IVIVE data. The methods are generalizable to other enzymes involved in drug metabolism. These are important for continuous improvements to PBPK simulations in the development of new drugs. As this case study for UGTs illustrates, accurate estimates of functional enzyme kinetics in various tissues are still limited. It would be desirable to conduct functional assays on the same samples as proteomic measurements to confirm the preliminary findings presented here. Nevertheless, our results suggest that k_{cat} may vary from tissue to tissue, perhaps even within similar tissues depending upon disease state.

Authorship Contributions

Participated in research design: Ahmed, Rostami-Hodjegan, Al-Majdoub.

Performed data analysis: Ahmed.

Wrote or contributed to the writing of the manuscript: Ahmed, Rostami-Hodjegan, Barber, Al-Majdoub.

References

Achour B, Dantonio A, Niosi M, Novak JJ, Al-Majdoub ZM, Goosen TC, Rostami-Hodjegan A, and Barber J (2018) Data generated by quantitative liquid chromatography-mass spectrometry proteomics are only the start and not the endpoint: optimization of quantitative concatemer-based measurement of hepatic uridine-5′-diphosphate-glucuronosyltransferase enzymes with reference to catalytic activity. *Drug Metab Dispos* **46**:805–812.

Achour B, Dantonio A, Niosi M, Novak JJ, Fallon JK, Barber J, Smith PC, Rostami-Hodjegan A, and Goosen TC (2017) Quantitative characterization of major hepatic UDP-glucuronosyltransferase enzymes in human liver microsomes: comparison of two proteomic methods and correlation with catalytic activity. *Drug Metab Dispos* **45**:1102–1112.

Achour B, Rostami-Hodjegan A, and Barber J (2014) Protein expression of various hepatic uridine 5′-diphosphate glucuronosyltransferase (UGT) enzymes and their inter-correlations: a meta-analysis. *Biopharm Drug Dispos* **35**:353–361.

Al-Jahdari WS, Yamamoto K, Hiraoka H, Nakamura K, Goto F, and Horiuchi R (2006) Prediction of total propofol clearance based on enzyme activities in microsomes from human kidney and liver. *Eur J Clin Pharmacol* **62**:527–533.

Al-Majdoub ZM, Scotcher D, Achour B, Barber J, Galetin A, and Rostami-Hodjegan A (2021) Quantitative proteomic map of enzymes and transporters in the human kidney: stepping closer to mechanistic kidney models to define local kinetics. *Clin Pharmacol Ther* **110**:1389–1400.

Argikar UA, Potter PM, Hutzler JM, and Marathe PH (2016) Challenges and opportunities with non-CYP enzymes aldehyde oxidase, carboxylesterase, and UDP-glucuronosyltransferase: focus on reaction phenotyping and prediction of human clearance. *AAPS J* **18**:1391–1405.

Badée J, Qiu N, Parrott N, Collier AC, Schmidt S, and Fowler S (2019) Optimization of experimental conditions of automated glucuronidation assays in human liver microsomes using a cocktail approach and ultra-high performance liquid chromatography-tandem mass spectrometry. *Drug Metab Dispos* **47**:124–134.

Benoit-Biancamano MO, Connelly J, Villeneuve L, Caron P, and Guillemette C (2009) Deferiprone glucuronidation by human tissues and recombinant UDP glucuronosyltransferase 1A6: an in vitro investigation of genetic and splice variants. *Drug Metab Dispos* **37**:322–329.

Bhatt DK, Mehrotra A, Gaedigk A, Chapa R, Basit A, Zhang H, Choudhari P, Boberg M, Pearce RE, Gaedigk R, et al. (2019) Age- and genotype-dependent variability in the protein abundance and activity of six major uridine diphosphate-glucuronosyltransferases in human liver. *Clin Pharmacol Ther* **105**:131–141.

Chen A, Zhou X, Cheng Y, Tang S, Liu M, and Wang X (2018) Design and optimization of the cocktail assay for rapid assessment of the activity of UGT enzymes in human and rat liver microsomes. *Toxicol Lett* **295**:379–389.

Couto N, Al-Majdoub ZM, Gibson S, Davies PJ, Achour B, Harwood MD, Carlson G, Barber J, Rostami-Hodjegan A, and Warhurst G (2020) Quantitative proteomics of clinically relevant drug-metabolizing enzymes and drug transporters and their intercorrelations in the human small intestine. *Drug Metab Dispos* **48**:245–254.

Crewe HK, Barter ZE, Yeo KR, and Rostami-Hodjegan A (2011) Are there differences in the catalytic activity per unit enzyme of recombinantly expressed and human liver microsomal cytochrome P450 2C9? A systematic investigation into inter-system extrapolation factors. *Biopharm Drug Dispos* **32**:303–318.

Cubitt HE, Houston JB, and Galetin A (2009) Relative importance of intestinal and hepatic glucuronidation-impact on the prediction of drug clearance. *Pharm Res* **26**:1073–1083.

El-Khateeb E, Burkhill S, Murby S, Amirat H, Rostami-Hodjegan A, and Ahmad A (2021) Physiological-based pharmacokinetic modeling trends in pharmaceutical drug development over the last 20-years; in-depth analysis of applications, organizations, and platforms. *Biopharm Drug Dispos* **42**:107–117.

Galetin A and Houston JB (2006) Intestinal and hepatic metabolic activity of five cytochrome P450 enzymes: impact on prediction of first-pass metabolism. *J Pharmacol Exp Ther* **318**:1220–1229.

Gao H, Yao L, Mathieu HW, Zhang Y, Maurer TS, Troutman MD, Scott DO, Ruggeri RB, and Lin J (2008) In silico modeling of nonspecific binding to human liver microsomes. *Drug Metab Dispos* **36**:2130–2135.

Gill KL, Gertz M, Houston JB, and Galetin A (2013) Application of a physiologically based pharmacokinetic model to assess propofol hepatic and renal glucuronidation in isolation: utility of in vitro and in vivo data. *Drug Metab Dispos* **41**:744–753.

Gill KL, Houston JB, and Galetin A (2012) Characterization of in vitro glucuronidation clearance of a range of drugs in human kidney microsomes: comparison with liver and intestinal glucuronidation and impact of albumin. *Drug Metab Dispos* **40**:825–835.

Hallifax D and Houston JB (2006) Binding of drugs to hepatic microsomes: comment and assessment of current prediction methodology with recommendation for improvement. *Drug Metab Dispos* **34**:724–726, author reply 727.

Howard M, Barber J, Alizai N, and Rostami-Hodjegan A (2018) Dose adjustment in orphan disease populations: the quest to fulfill the requirements of physiologically based pharmacokinetics. *Expert Opin Drug Metab Toxicol* **14**:1315–1330.

Knights KM, Spencer SM, Fallon JK, Chau N, Smith PC, and Miners JO (2016) Scaling factors for the in vitro-in vivo extrapolation (IV-IVE) of renal drug and xenobiotic glucuronidation clearance. *Br J Clin Pharmacol* **81**:1153–1164.

Komura H and Iwaki M (2011) In vitro and in vivo small intestinal metabolism of CYP3A and UGT substrates in preclinical animals species and humans: species differences. *Drug Metab Rev* **43**:476–498.

Liang S-C, Ge G-B, Liu H-X, Shang H-T, Wei H, Fang Z-Z, Zhu L-L, Mao Y-X, and Yang L (2011) Determination of propofol UDP-glucuronosyltransferase (UGT) activities in hepatic microsomes from different species by UFLC-ESI-MS. *J Pharm Biomed Anal* **54**:236–241.

Miles KK, Stern ST, Smith PC, Kessler FK, Ali S, and Ritter JK (2005) An investigation of human and rat liver microsomal mycophenolic acid glucuronidation: evidence for a principal role of UGT1A enzymes and species differences in UGT1A specificity. *Drug Metab Dispos* **33**:1513–1520.

Miners JO, Rowland A, Novak JJ, Lapham K, and Goosen TC (2021) Evidence-based strategies for the characterisation of human drug and chemical glucuronidation in vitro and UDP-glucuronosyltransferase reaction phenotyping. *Pharmacol Ther* **218**:107689.

Nishimura T, Amano N, Kubo Y, Ono M, Kato Y, Fujita H, Kimura Y, and Tsuji A (2007) Asymmetric intestinal first-pass metabolism causes minimal oral bioavailability of midazolam in cynomolgus monkey. *Drug Metab Dispos* **35**:1275–1284.

Pang KS, Han YR, Noh K, Lee PI, and Rowland M (2019) Hepatic clearance concepts and misconceptions: why the well-stirred model is still used even though it is not physiologic reality? *Biochem Pharmacol* **169**:113596.

Picard N, Ratanasavanh D, Prémaud A, Le Meur Y, and Marquet P (2005) Identification of the UDP-glucuronosyltransferase isoforms involved in mycophenolic acid phase II metabolism. *Drug Metab Dispos* **33**:139–146.

Robinson PK (2015) Enzymes: principles and biotechnological applications. *Essays Biochem* **59**:1–41.

Rowland A, Knights KM, Mackenzie PI, and Miners JO (2008) The "albumin effect" and drug glucuronidation: bovine serum albumin and fatty acid-free human serum albumin enhance the glucuronidation of UDP-glucuronosyltransferase (UGT) 1A9 substrates but not UGT1A1 and UGT1A6 activities. *Drug Metab Dispos* **36**:1056–1062.

Scotcher D, Billington S, Brown J, Jones CR, Brown CDA, Rostami-Hodjegan A, and Galetin A (2017) Microsomal and cytosolic scaling factors in dog and human kidney cortex and application for in vitro-in vivo extrapolation of renal metabolic clearance. *Drug Metab Dispos* **45**:556–568.

Scotcher D, Jones C, Posada M, Galetin A, and Rostami-Hodjegan A (2016) Key to opening kidney for in vitro-in vivo extrapolation entrance in health and disease: part II: mechanistic models and in vitro-in vivo extrapolation. *AAPS J* **18**:1082–1094.

Seo KA, Kim HJ, Jeong ES, Abdalla N, Choi CS, Kim DH, and Shin JG (2014) In vitro assay of six UDP-glucuronosyltransferase isoforms in human liver microsomes, using cocktails of probe substrates and liquid chromatography-tandem mass spectrometry. *Drug Metab Dispos* **42**:1803–1810.

Shimizu M, Matsumoto Y, and Yamazaki H (2007) Effects of propofol analogs on glucuronidation of propofol, an anesthetic drug, by human liver microsomes. *Drug Metab Lett* **1**:77–79.

Soars MG, Riley RJ, Findlay KAB, Coffey MJ, and Burchell B (2001) Evidence for significant differences in microsomal drug glucuronidation by canine and human liver and kidney. *Drug Metab Dispos* **29**:121–126.

Soars MG, Ring BJ, and Wrighton SA (2003) The effect of incubation conditions on the enzyme kinetics of udp-glucuronosyltransferases. *Drug Metab Dispos* **31**:762–767.

Stingl JC, Bartels H, Viviani R, Lehmann ML, and Brockmöller J (2014) Relevance of UDP-glucuronosyltransferase polymorphisms for drug dosing: a quantitative systematic review. *Pharmacol Ther* **141**:92–116.

von Richter O, Burk O, Fromm MF, Thon KP, Eichelbaum M, and Kivistö KT (2004) Cytochrome P450 3A4 and P-glycoprotein expression in human small intestinal enterocytes and hepatocytes: a comparative analysis in paired tissue specimens. *Clin Pharmacol Ther* **75**:172–183.

Walsky RL, Bauman JN, Bourcier K, Giddens G, Lapham K, Negahban A, Ryder TF, Obach RS, Hyland R, and Goosen TC (2012) Optimized assays for human UDP-glucuronosyltransferase (UGT) activities: altered alamethicin concentration and utility to screen for UGT inhibitors. *Drug Metab Dispos* **40**:1051–1065.

Wu B, Dong D, Hu M, and Zhang S (2013) Quantitative prediction of glucuronidation in humans using the in vitro- in vivo extrapolation approach. *Curr Top Med Chem* **13**:1343–1352.

Yang J, Tucker GT, and Rostami-Hodjegan A (2004) Cytochrome P450 3A expression and activity in the human small intestine. *Clin Pharmacol Ther* **76**:391.

Address correspondence to: Dr. Zubida Al-Majdoub, Centre for Applied Pharmacokinetic Research, University of Manchester, Room 3.32, Stopford Building, Oxford Road, Manchester M13 9PT, UK. E-mail: zubida.al-majdoub@manchester.ac.uk